

# Removal of Ni<sup>2+</sup> from aqueous solutions by adsorption onto magnetic multiwalled carbon nanotube nanocomposite

Wojciech Konicki<sup>1\*</sup>, Iwona Pelech<sup>2</sup>, Ewa Mijowska<sup>2</sup>

<sup>1</sup> Maritime University of Szczecin, Department of Integrated Transport Technology and Environmental Protection, Henryka Pobożnego 11, 70-507 Szczecin, Poland

<sup>2</sup> West Pomeranian University of Technology, Szczecin, Institute of Chemical and Environment Engineering, Pułaskiego 10, 70-322 Szczecin, Poland

\*Corresponding author: e-mail: w.konicki@am.szczecin.pl

The removal of Ni<sup>2+</sup> from aqueous solution by magnetic multiwalled carbon nanotube nanocomposite (MMWCNTs-C) was investigated. MMWCNTs-C was characterized by X-ray Diffraction method (XRD), High-Resolution Transmission Electron Microscopy (HRTEM), surface area (BET), and Fourier Transform-Infrared Spectroscopy (FTIR). The effects of initial concentration, contact time, solution pH, and temperature on the Ni<sup>2+</sup> adsorption onto MMWCNTs-C were studied. The Langmuir and Freundlich isotherm models were applied to fit the adsorption data. The results showed that the adsorption isotherm data were fitted well to the Langmuir isotherm model with the maximum monolayer adsorption capacity of 2.11 mg g<sup>-1</sup>. The adsorption kinetics was best described by the pseudo-second-order model. The thermodynamic parameters, such as  $\Delta H^\circ$ ,  $\Delta G^\circ$  and  $\Delta S^\circ$ , were also determined and evaluated. The adsorption of Ni<sup>2+</sup> is generally spontaneous and thermodynamically favorable. The values of  $\Delta H^\circ$  and  $\Delta G^\circ$  indicate that the adsorption of Ni<sup>2+</sup> onto MMWCNTs-C was a physisorption process.

**Keywords:** magnetic nanocomposite, multiwalled carbon nanotubes, nickel, adsorption.

## INTRODUCTION

Nickel is the one of the important toxic heavy metals. It is used in a wide range of manufacturing industries, such as metal plating, galvanizing, smelting, mining, pigment and ceramics industries and is present in the wastewaters. Nickel is non-biodegradable metal and may cause dermatitis and allergic sensitization. At higher concentrations it is a potent carcinogen and causes cancer of lungs, nose and bone<sup>1</sup>. Therefore, it is necessary to remove nickel from various industrial effluents.

Various techniques such as ion exchange, membrane filtration, reverse osmosis, precipitation and adsorption have been proposed for the removal of nickel from aqueous solutions. Among these techniques, the adsorption process has been widely applied to remove heavy metal ions from aqueous solutions because of its simplicity and cost effectiveness. In recent years, a number of different adsorbents such as spent animal bones<sup>2</sup>, crab shell<sup>3</sup>, seaweeds<sup>4</sup>, nanoparticle Fe<sub>3</sub>O<sub>4</sub> impregnated onto tea waste<sup>5</sup>, activated carbon<sup>6</sup>, olive stone waste<sup>7</sup> and fly ash<sup>8</sup> have been reported for the removal of Ni<sup>2+</sup> from aqueous solutions.

Carbon nanotubes CNTs, as a new form of carbon, are attracting great research interest due to their extraordinary chemical, mechanical and electrical property. Their small size, hollow and layered nanosized structures make them a good candidate as adsorbents for removing many kinds of inorganic contaminants such as heavy metal ions (Cd<sup>2+</sup>, Pb<sup>2+</sup>, Zn<sup>2+</sup>, Co<sup>2+</sup>, Cu<sup>2+</sup>)<sup>9, 10</sup>.

However, to date only four studies have been conducted on the adsorption of Ni<sup>2+</sup> by CNTs. Gao et al. have investigated the adsorption of Ni<sup>2+</sup>, Cu<sup>2+</sup>, Zn<sup>2+</sup> and Cd<sup>2+</sup> from aqueous solutions on carbon nanotubes in single, binary, ternary and quaternary systems<sup>11</sup>. Kandah and Meunier have studied the adsorption capacity of the as-produced and oxidized CNTs on adsorption of nickel ions from aqueous solutions<sup>12</sup>. Yang et al.<sup>13</sup> have investigated the adsorption of Ni<sup>2+</sup> on oxidized

multiwalled carbon nanotubes. Chen et al. have prepared multiwall carbon nanotube/iron oxide magnetic composite for removal of Ni<sup>2+</sup> and Sr<sup>2+</sup> from aqueous solutions<sup>14</sup>. Unfortunately, the separation of carbon nanotubes from solution is very difficult and thus severely restricts water treatment applications. Compared with traditional methods, the magnetic separation method is considered as a relatively simple, fast and effective technique for separating adsorbents from solutions. Despite these facts, only a very few studies have been conducted on the adsorption of heavy metal ions by magnetic CNTs. Jeon et al.<sup>15</sup> have synthesized magnetic alginate/CNT/maghemite composite as adsorbent for the removal of Cu<sup>2+</sup> in aqueous pollutant. Gupta et al.<sup>16</sup> have studied the adsorption of Cr<sup>3+</sup> onto magnetic multiwall carbon nanotubes/ nano-iron oxide composite. Ma et al.<sup>17</sup> have investigated the adsorption of arsenic onto magnetic iron oxide/CNTs composite. Peng et al.<sup>18</sup> used CNTs/iron oxides magnetic composites as adsorbent for removal of Pb<sup>2+</sup> and Cu<sup>2+</sup> from water.

Therefore, in this work, magnetic multiwalled carbon nanotube nanocomposite (MMWCNTs-C) was used for the removal of Ni<sup>2+</sup> from aqueous solution. The main advantage is that the adsorbent can be easily and simply separated using the external magnetic field. The effects of pH, temperature and initial dye concentration on Ni<sup>2+</sup> adsorption by the MMWCNTs-C were investigated. The experimental data were analyzed using the pseudo-first-order and the pseudo-second-order kinetic model. Langmuir and Freundlich isotherms were employed to quantify the adsorption equilibrium. Thermodynamics parameters,  $\Delta G^\circ$ ,  $\Delta H^\circ$  and  $\Delta S^\circ$ , were also calculated.

## EXPERIMENTAL

### Material and characterization methods

Analytical grade nickel standard solution (Ion Standard Solution of 1000 mg L<sup>-1</sup>) was purchased from Merck

and was employed to prepare stock solution containing  $100 \text{ mg L}^{-1}$  of  $\text{Ni}^{2+}$ . The stock solution was then further diluted to the desired concentrations. Dimethylglyoxime was obtained from Fluka. Magnetic multiwalled carbon nanotubes nanocomposite material MMWCNTs-C was prepared by chemical vapor deposition CVD method using ethylene as a carbon source. As a catalyst nanocrystalline iron was applied. Nanocrystalline iron was obtained by fusion of magnetite with small amounts of promoter oxides ( $\text{Al}_2\text{O}_3$  and  $\text{CaO}$ ), followed by reduction with hydrogen. The synthesis of carbon material was conducted in the high temperature furnace (Carbolite STF 16/800). 1 g of catalyst was placed in a quartz boat inside the furnace. In the first stage the catalyst was reduced polythermally at the temperature raising from  $20^\circ\text{C}$  to  $500^\circ\text{C}$  and next isothermally at  $500^\circ\text{C}$  for 1 h. The reduction process was carried out in order to remove a thin passivation layer. In the second stage, the synthesis of nanocomposite was performed under mixture of ethylene and argon (1:1, total flow 40 l/h) at  $700^\circ\text{C}$  for 1 h. Next the sample was cooled to the room temperature under argon flow (10 l/h). Details of the nanocrystalline iron and magnetic nanocomposite preparation are given in work<sup>19</sup>.

The phase composition of the MMWCNTs-C was determined using the X-ray diffraction method (X'Pert PRO Philips diffractometer) using a  $\text{CuK}\alpha$  radiation. The amount of iron in the MMWCNTs-C was determined using thermogravimetric analysis which was performed on DTA-Q600 SDT TA Instruments. The morphology of the adsorbent was investigated by high-resolution transmission electron microscopy HRTEM using a FEI Tecnai F20. The MMWCNTs-C was analyzed for their BET-specific surface area and pore-size distribution using an Quadrasorb SI Quantachrome analyzer. The functional groups on the MMWCNTs-C surface were determined using fourier transform infrared FTIR method (Perkin Elmer Spectrum One FT-IR spectrometer). The  $\text{pH}_{\text{PZC}}$  (point of zero charge) is a critical value for determining quantitatively the net charge carried on the adsorbent surface as a function of the solution pH. Point of zero charge of MMWCNTs-C was determined by the pH drift method<sup>20</sup>. For this purpose, 50 ml of a 0.01M NaCl solution was placed in a closed Erlenmeyer flask and the pH was adjusted to a value between 3.1 and 12.4 by the addition of 0.1M HCl or 0.1M NaOH. Then, 0.15 g of MMWCNTs-C was added to the solution and the final pH measured after 48 h under agitation at room temperature. The  $\text{pH}_{\text{PZC}}$  of MMWCNTs-C was obtained from the plot of  $\Delta\text{pH} = \text{pH}_i - \text{pH}_f$  (the difference between initial  $\text{pH}_i$  and final  $\text{pH}_f$  at equilibrium) versus initial  $\text{pH}_i$ . The point of intersection of the resulting curve at which  $\Delta\text{pH} = 0$  gave the  $\text{pH}_{\text{PZC}}$ . All chemicals used in the experiments were purchased in analytical purity and used without any purification. All solutions were prepared with deionized water.

### Adsorption experiments

Adsorption experiments were carried out in Erlenmeyer flask, where the solution (200 mL) with the initial  $\text{Ni}^{2+}$  concentration of  $0.82\text{--}4.12 \text{ mg L}^{-1}$  was placed. The flask with  $\text{Ni}^{2+}$  solution was sealed and placed in a constant temperature bath and agitated with a magnetic stirrer in

order to achieve homogeneity. To observe the effect of temperature the experiments were carried out at three different temperatures, i.e., 20, 40 and  $60^\circ\text{C}$ . Before mixing with the adsorbent, various pH levels (3.5–11.2) of the solution was adjusted by adding a few drops of diluted hydrochloric acid (0.1N HCl) or sodium hydroxide (0.1N NaOH). When the desired temperature was reached, about 0.15 g of MMWCNTs-C was added into flask. Next, the flask with suspension was placed in the ultrasonic bath (Raypa UCI-50) at the same temperature. MMWCNTs were dispersed into the dye solution by sonication for 1 min and then flask with suspension was placed in a constant temperature bath and intensively mixed by magnetic stirrer. At the end of the equilibrium period 4 ml of aqueous sample was taken from the solution, and the liquid was separated from the adsorbent magnetically. The concentration of  $\text{Ni}^{2+}$  was analyzed by UV-VIS spectrophotometer at 530 nm using the dimethylglyoxime method<sup>21</sup>. The amount of  $\text{Ni}^{2+}$  adsorbed at equilibrium  $q_e$  ( $\text{mg g}^{-1}$ ) was calculated by the following equation:

$$q_e = \frac{(C_0 - C_e)V}{m} \quad (1)$$

where:  $C_0$  ( $\text{mg L}^{-1}$ ) is the initial  $\text{Ni}^{2+}$  concentration,  $C_e$  ( $\text{mg L}^{-1}$ ) the  $\text{Ni}^{2+}$  concentration at equilibrium,  $V$  (L) the volume of the solution and  $m$  (g) is the mass of the adsorbent.

The procedures of kinetic experiments were identical with those of equilibrium tests. At predetermined moments, aqueous samples were taken from the solution, the liquid was separated from the adsorbent and concentration of  $\text{Ni}^{2+}$  in solution was determined spectrophotometrically. The amount of  $\text{Ni}^{2+}$  adsorbed at time  $t$   $q_t$  ( $\text{mg g}^{-1}$ ) was calculated by following equation:

$$q_t = \frac{(C_0 - C_t)V}{m} \quad (2)$$

where:  $C_t$  ( $\text{mg L}^{-1}$ ) the  $\text{Ni}^{2+}$  concentration at any time  $t$ . Each experiment was carried out in duplicate and the average results are presented. The kinetic and isotherm models were evaluated by the linear correlation coefficient ( $R^2$ ).

## RESULTS AND DISCUSSION

### Characterization of the adsorbent

Figure 1 shows the X-ray diffraction pattern of nanocrystalline iron before decomposition of ethylene and MMWCNTs-C. According to the data acquired from the XRD, nanocomposite MMWCNTs-C consisted of graphite (peak at 2 values of 26.232) and iron carbide  $\text{Fe}_3\text{C}$  (reference standard JCPDS file 35-0772) phase only. The iron oxide or iron particles in MMWCNTs-C were not detected. Iron content measured by TGA in the MMWCNTs-C was about 16%. The morphological structure and arrangement of multiwalled carbon nanotubes are shown in Figure 2a and b. Iron carbide particles were observed at the tip of carbon nanotubes (Fig. 2c). Iron carbide ( $\text{Fe}_3\text{C}$ ) is ferromagnetic at room temperature. This allowed for an easy removal of nanocomposite from aqueous solution by external magnetic field. Inset of Figure 2c shows the suspension of MMWCNTs-C and separation of the adsorbent from solution with a magnet.

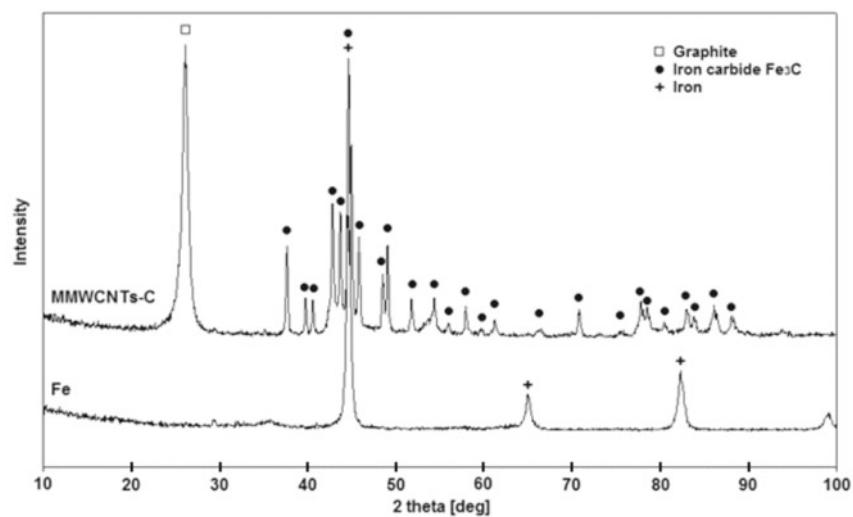


Figure 1. X-ray diffraction pattern of nanocrystalline iron and MMWCNTs-C

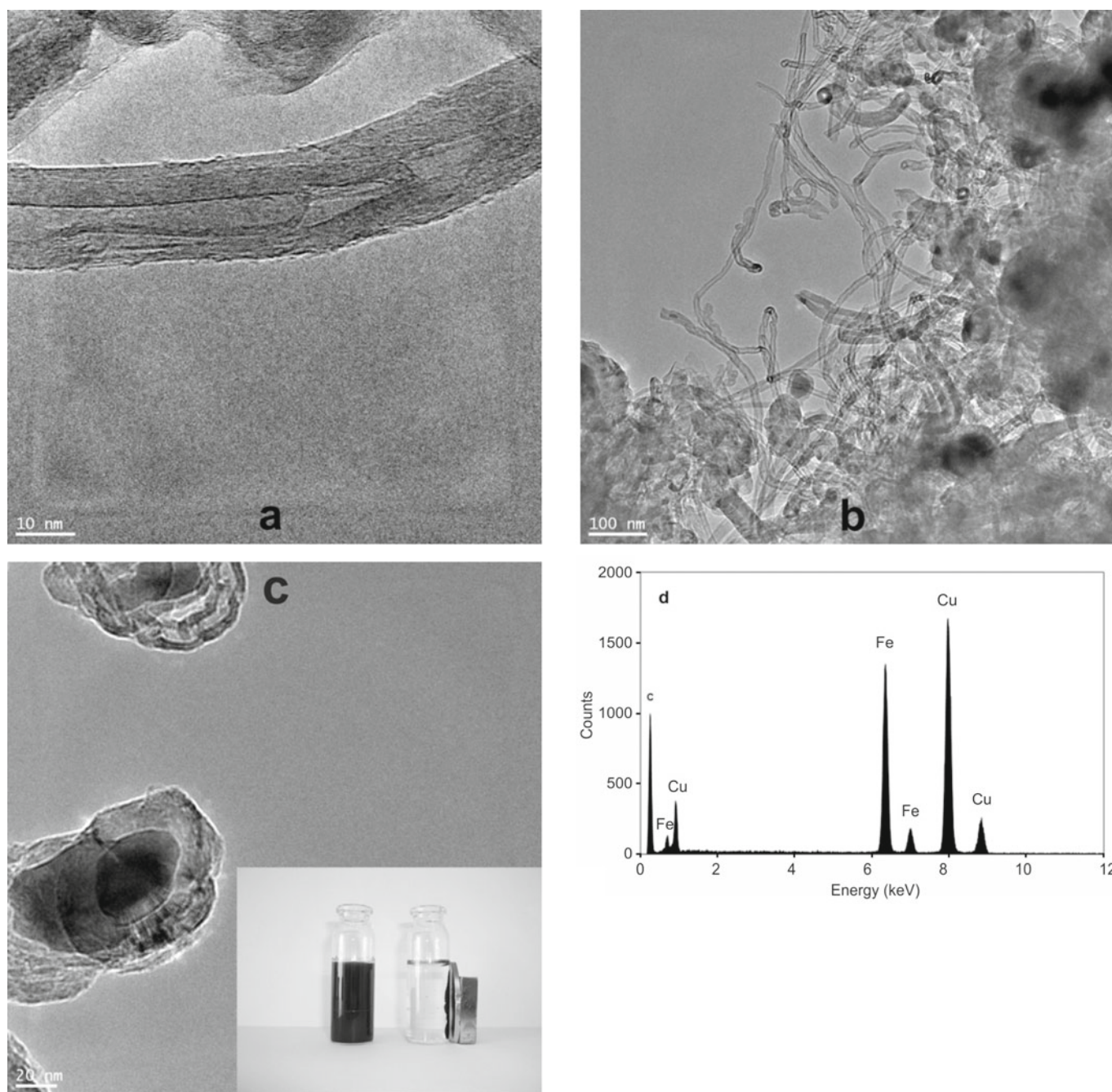


Figure 2. HRTEM images of MMWCNTs-C: (a) Structure of multiwalled carbon nanotubes, (b) Full picture of MMWCNTs-C, (c) Iron carbide particles; Inset: separation of the MMWCNTs-C from the aqueous solution with a magnet, (d) EDX spectrum of MMWCNTs-C

Figure 2d shows an EDX spectrum of MMWCNTs-C which reveals the presence of carbon from the multiwalled carbon nanotubes and iron from the  $\text{Fe}_3\text{C}$ . The Cu peaks were from the copper grid. The BET surface area was found to be  $38.7 \text{ m}^2 \text{ g}^{-1}$  and the total pore volume was  $0.27 \text{ cm}^3 \text{ g}^{-1}$ . The FTIR measurement of MMWCNTs-C showed the presence of the following functional groups: -COOH and -C=C. The  $\text{pH}_{\text{PZC}}$  of MMWCNTs-C was found to be 10.6 (Fig. 3). This value refers to the pH level at which the surface of the MMWCNTs-C has zero net charge. At  $\text{pH} < \text{pH}_{\text{PZC}}$ , the MMWCNTs-C surface has a net positive charge and adsorption of anions is favored, while at  $\text{pH} > \text{pH}_{\text{PZC}}$  the surface has a net negative charge and adsorption of cations is favored. The characterization of the adsorbent has been described in detail elsewhere<sup>22</sup>.

### Adsorption kinetics

The effect of initial concentration of  $\text{Ni}^{2+}$  on its removal from aqueous solutions by MMWCNTs-C at  $30^\circ\text{C}$  is presented in Fig. 4. The initial concentration was varied from 0.82 to  $4.12 \text{ mg L}^{-1}$ . The adsorption of the  $\text{Ni}^{2+}$  onto MMWCNTs-C increased with time and then attained equilibrium. The adsorption is very fast initially and then slow. The initial concentration provides an important driving force to overcome all mass transfer resistances of the  $\text{Ni}^{2+}$  between the aqueous solution and solid phases. The adsorption capacity at equilibrium increases evidently from 0.88 to  $1.95 \text{ mg g}^{-1}$ , with an

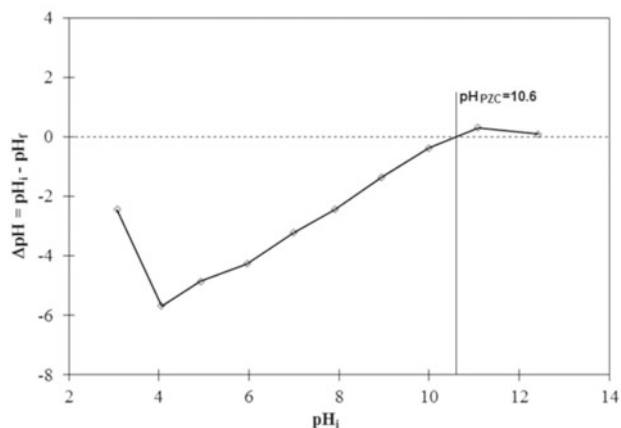


Figure 3.  $\text{pH}_{\text{PZC}}$  point of zero charge of MMWCNTs-C

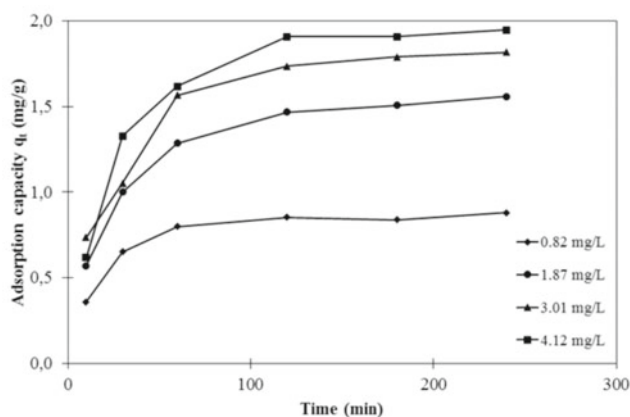


Figure 4. The effect of initial concentration of  $\text{Ni}^{2+}$  on adsorption capacity onto MMWCNTs-C (Experimental conditions:  $T = 30^\circ\text{C}$ ,  $\text{pH} = 7$ )

increase in the initial concentration of  $\text{Ni}^{2+}$  from 0.82 to  $4.12 \text{ mg L}^{-1}$ .

In this study the kinetics of the adsorption of  $\text{Ni}^{2+}$  on MMWCNTs-C have been described by the pseudo-first-order and pseudo-second-order kinetic models. The pseudo-first-order model is represented by the following equation<sup>23</sup>:

$$\ln(q_e - q_t) = \ln q_e - k_1 t \quad (3)$$

where  $q_e$  ( $\text{mg g}^{-1}$ ) is the amount of  $\text{Ni}^{2+}$  adsorbed per unit mass of adsorbent at equilibrium,  $q_t$  ( $\text{mg g}^{-1}$ ) is the amount of  $\text{Ni}^{2+}$  adsorbed per unit mass of adsorbent at any time  $t$  (min) and  $k_1$  ( $\text{min}^{-1}$ ) is the first-order rate constant adsorption. Values of  $k_1$  and equilibrium adsorption density  $q_e$  at  $30^\circ\text{C}$  were calculated from the plots of  $\ln(q_e - q_t)$  versus  $t$  for different initial concentrations of  $\text{Ni}^{2+}$  (Fig. 5a). The pseudo-second-order kinetic model can be expressed as follows:

$$\frac{t}{q_t} = \frac{1}{k_2 q_e^2} + \frac{1}{q_e} t \quad (4)$$

where  $k_2$  ( $\text{g mg}^{-1} \text{ min}^{-1}$ ) is the rate constant for the pseudo-second-order adsorption kinetics. Values of  $k_2$  and  $q_e$  for different initial concentrations of  $\text{Ni}^{2+}$  were calculated from the slope and intercept of the linear plot of  $t/q_t$  versus  $t$ . The plot of  $t/q_t$  versus  $t$  at  $30^\circ\text{C}$ , is shown in Figure 5b. The results of the kinetic data are listed in Table 1. Based on the correlation coefficients, it can be said that the adsorption fits to the pseudo-second-order ( $R^2 = 0.998 \div 1$ ) better than the pseudo-first-order kinetic model ( $R^2 = 0.790 \div 0.983$ ). Also, the calculated  $q_{e,\text{cal}}$  values from the pseudo-second-order model were very close to the experimental  $q_{e,\text{exp}}$  values. The results indicated that the adsorption fits to the pseudo-second-order kinetic model better than the pseudo-first-order. Similar kinetic results were also observed in the adsorption of  $\text{Ni}^{2+}$  on oxidized multi-walled carbon nanotubes<sup>13</sup> and bael tree leaf powder<sup>24</sup>. From Table 1, it was also observed that the pseudo-second-order rate constant  $k_2$  decreased from  $0.0874$  to  $0.0240 \text{ g mg}^{-1} \text{ min}^{-1}$ , as the initial concentration of  $\text{Ni}^{2+}$  increased from 0.82 to  $4.12 \text{ mg L}^{-1}$ .

### Adsorption isotherms

Adsorption isotherms are important for the description how molecules of adsorbate interact with adsorbent surface sites. In this study, the Langmuir and Freundlich isotherms were used to describe the equilibrium adsorption. The Langmuir's isotherm model is represented by the following linear equation<sup>25</sup>:

$$\frac{C_e}{q_e} = \frac{1}{Q_0 b} + \frac{C_e}{Q_0} \quad (5)$$

where  $C_e$  ( $\text{mg L}^{-1}$ ) is the equilibrium concentration of the adsorbate,  $q_e$  ( $\text{mg g}^{-1}$ ) is the amount of adsorbate adsorbed per unit mass of adsorbent at equilibrium,  $Q_0$  ( $\text{mg g}^{-1}$ ) is the monolayer adsorption capacity and  $b$  ( $\text{L mg}^{-1}$ ) is a constant related to energy of adsorption. The values of  $Q_0$  and  $b$  were calculated from the slope and intercept of the linear plot  $C_e/q_e$  versus  $C_e$ . The plot of  $C_e/q_e$  versus  $C_e$  at  $30^\circ\text{C}$  is shown in Fig. 6a. The essential characteristics of the Langmuir isotherm can be expressed in terms of a dimensionless equilibrium parameter ( $R_L$ ), which is defined by the following equation:

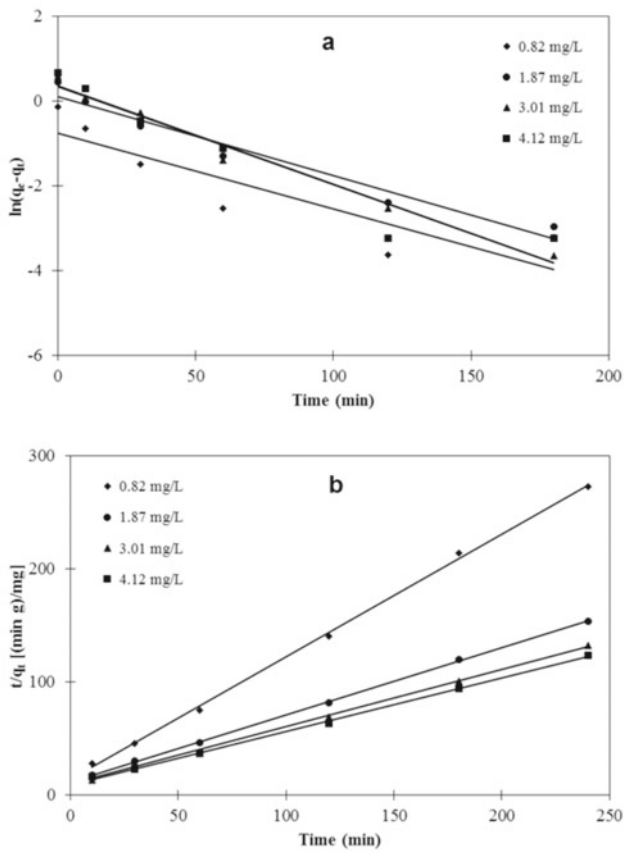


**Figure 5.** Pseudo-first-order kinetics (a) and pseudo-second-order kinetics, (b) of adsorption  $\text{Ni}^{2+}$  onto MMWCNTs-C at  $30^\circ\text{C}$

$$R_L = \frac{1}{1 + bC_0} \quad (6)$$

where:  $b$  ( $\text{L mg}^{-1}$ ) is the Langmuir constant and  $C_0$  ( $\text{mg L}^{-1}$ ) is the highest initial concentration of the adsorbate. The value of  $R_L$  indicates the type of the isotherm to be either unfavorable ( $R_L > 1$ ), linear ( $R_L = 1$ ), favorable ( $0 < R_L < 1$ ) or irreversible ( $R_L = 0$ ). The values of  $R_L$  was found to be 0.054 and confirmed that the MMWCNTs-C is favorable for adsorption of  $\text{Ni}^{2+}$  under the conditions used in this study.

The well-known logarithmic form of Freundlich model is represented by the following equation:

$$\ln q_e = \ln K_F + \left(\frac{1}{n}\right) \ln C_e \quad (7)$$

where:  $q_e$  ( $\text{mg g}^{-1}$ ) is the amount of adsorbate adsorbed per unit mass of adsorbent at equilibrium,  $K_F$  ( $\text{mg g}^{-1}(\text{L mg}^{-1})^{1/n}$ ) and  $n$  are Freundlich constants, which represent adsorption capacity and adsorption strength, respectively and  $C_e$  ( $\text{mg L}^{-1}$ ) is the equilibrium concentration of the adsorbate. The values of  $K_F$  and  $n$  were calculated from the slope and intercept of the linear plot  $\ln q_e$  versus  $\ln C_e$  (Fig. 6b). Table 2 showed the values of Langmuir and Freundlich constants, and the correlation coefficients

$R^2$  obtained from the linear regression. As seen, the experimental data better fit Langmuir model ( $R^2 = 1$ ) than the Freundlich model ( $R^2 = 0.953$ ). The maximum monolayer adsorption capacity  $Q_0$  obtained from the Langmuir model was  $2.11 \text{ mg g}^{-1}$ . Table 3 lists and compares the maximum monolayer adsorption capacity of  $\text{Ni}^{2+}$  on various adsorbents.

### Effect of pH

The pH of the solution is a very important factor for the adsorption process of metal ions. The influence of initial pH solution on adsorption capacity at equilibrium of  $\text{Ni}^{2+}$  onto MMWCNTs-C was investigated in the range of pH values from 3.5 to 11.2 at a fixed  $\text{Ni}^{2+}$  concentration of  $3.01 \text{ mg L}^{-1}$  and  $30^\circ\text{C}$ . The effect of the initial pH on the adsorption capacity of  $\text{Ni}^{2+}$  is shown in Figure 7. The adsorption capacity increased when the pH of the solution was increased. The maximum adsorption capacity of  $\text{Ni}^{2+}$  was  $3.02 \text{ mg g}^{-1}$ , observed at pH 9.4. When the pH was increased from 9.4 to 11.2, the adsorption capacity of  $\text{Ni}^{2+}$  slightly decreased to  $2.89 \text{ mg g}^{-1}$ . The pHpzc of MMWCNTs-C was found to be 10.6. At  $\text{pH} < 10.6$ , the concentration of  $\text{H}^+$  ion is high, and the surface of the MMWCNTs-C becomes more positively charged, due to the protonation of electron

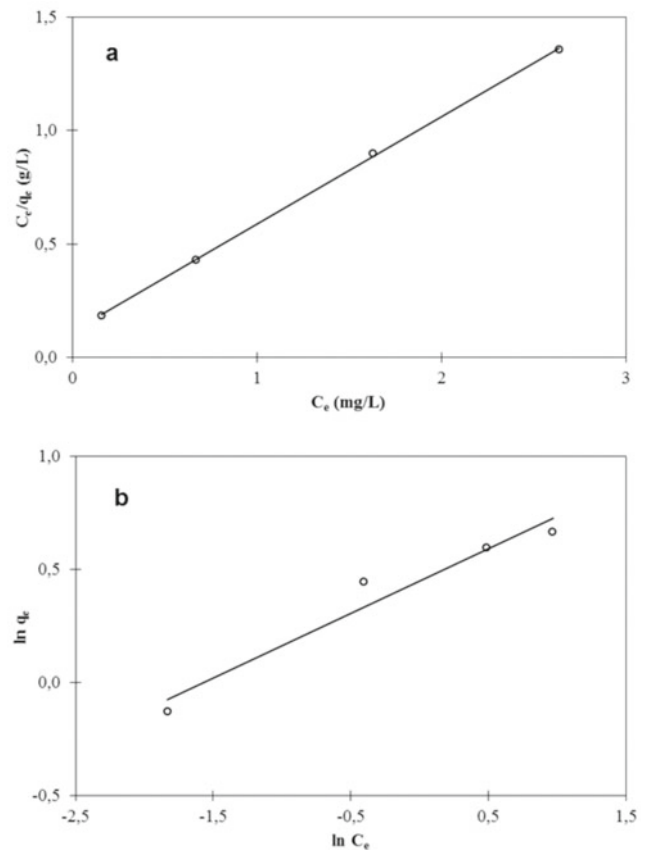


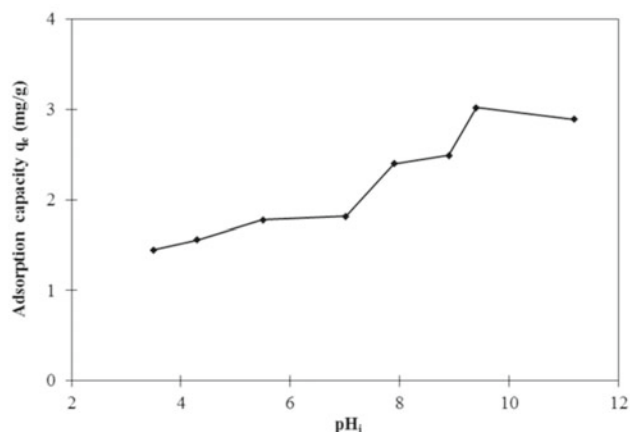
**Figure 6.** Langmuir (a) and Freundlich, (b) adsorption isotherm of  $\text{Ni}^{2+}$  onto MMWCNTs-C at  $30^\circ\text{C}$

**Table 1.** Comparison of the pseudo-first-order and pseudo-second-order kinetic models for different initial concentrations of  $\text{Ni}^{2+}$  at  $30^\circ\text{C}$

$C_0$ ( $\text{mg L}^{-1}$ )	$q_{e, \text{exp}}$ ( $\text{mg g}^{-1}$ )	Pseudo-first-order kinetic model			Pseudo-second-order kinetic model		
		$k_1$ ( $\text{min}^{-1}$ )	$q_{e, \text{cal}}$ ( $\text{mg g}^{-1}$ )	$R^2$	$k_2$ ( $\text{g mg}^{-1} \text{min}^{-1}$ )	$q_{e, \text{cal}}$ ( $\text{mg g}^{-1}$ )	$R^2$
0.82	0.88	0.0178	0.47	0.790	0.0874	0.92	0.999
1.87	1.56	0.0187	1.12	0.958	0.0308	1.68	1
3.01	1.82	0.0232	1.42	0.983	0.0267	1.97	0.998
4.12	1.95	0.0232	1.44	0.912	0.0240	2.13	0.998

**Table 2.** Langmuir and Freundlich parameters for the adsorption of the Ni<sup>2+</sup> on MMWCNTs-C at 30°C

Q <sub>0</sub> (mg g <sup>-1</sup> )	Langmuir isotherm			Freundlich isotherm		
	b (L mg <sup>-1</sup> )	R <sub>L</sub>	R <sup>2</sup>	K <sub>F</sub> [(mg g <sup>-1</sup> )(L mg <sup>-1</sup> ) <sup>1/n</sup> ]	n	R <sup>2</sup>
2.11	4.24	0.054	1	1.57	3.50	0.953

**Figure 7.** The effect of initial pH solution on adsorption Ni<sup>2+</sup> onto MMWCNTs-C (Experimental conditions: C<sub>Ni<sup>2+</sup></sub><sup>0</sup> = 3.01 mg L<sup>-1</sup>, T = 30°C)

$\pi$  rich regions on the surface of multiwalled carbon nanotubes. Additionally, at acidic pH, carboxylic groups are protonated to the cationic form (-COOH<sub>2</sub><sup>+</sup>). As the pH increases, the number of positively charged sites decreases and the number of negatively charged sites increases. A positively charged surface site does not favor the adsorption of Ni<sup>2+</sup> due to the electrostatic repulsion. At pH > 10.6 carboxylic groups dissociate to anionic form (-COO<sup>-</sup>) and generates electrostatic attraction force with Ni<sup>2+</sup>. However, in our study adsorption capacity of Ni<sup>2+</sup> decreased when the pH was increased from 9.4 to 11.2. Decrease in adsorption capacity at higher pH is probably due to aformation of soluble hydroxy complexes. Nickel is presents in the species of Ni<sup>2+</sup>, Ni(OH)<sup>+</sup>, Ni(OH)<sub>2</sub>, Ni(OH)<sub>3</sub><sup>-</sup> and Ni(OH)<sub>4</sub><sup>2-</sup> at different pH values<sup>13</sup>. At pH < 9, the predominant specie is Ni<sup>2+</sup>. With an increase in pH, the concentration of Ni<sup>2+</sup> ions decreases rapidly and increases the concentration of Ni(OH)<sup>+</sup>, Ni(OH)<sub>2</sub>

**Table 3.** Comparison of the maximum monolayer adsorption of Ni<sup>2+</sup> on various adsorbents

Adsorbent	Q <sub>0</sub> (mg g <sup>-1</sup> )	References
Bagasse	0.001	8
Fly ash	0.03	8
Aspergillus niger	1.10	26
Granular activated carbon	1.50	27
Oxidized CNTs	1.83	11
MMWCNTs-C	2.11	This study
Oxidized MWCNTs	3.73	13
Rice hull	5.75	28
Sheep manure waste	7.20	29
Deactivated protanated yeast	9.01	30
Peat moss	9.18	31
Coir pith	9.50	32
Calcium alginate	10.50	33
Fe <sub>3</sub> O <sub>4</sub>	11.53	34
Carbon aerogel	12.87	35

**Table 4.** Thermodynamic parameters for the adsorption of the Ni<sup>2+</sup> onto MMWCNTs-C

Ni <sup>2+</sup> concentration (mg L <sup>-1</sup> )	$\Delta H^{\circ}$ (kJ mol <sup>-1</sup> )	$\Delta S^{\circ}$ (J mol <sup>-1</sup> K <sup>-1</sup> )	$\Delta G^{\circ}$ at temperature (°C)		
			20	40	60
2.93	5.41	18.9	-103.6	-553.4	-852.9

and Ni(OH)<sub>3</sub><sup>-</sup>. Therefore, the adsorption of Ni<sup>2+</sup> onto MMWCNTs-C surface is lower at higher pH (basic pH).

### Effect of temperature

The effect of temperature on equilibrium adsorption of Ni<sup>2+</sup> onto MMWCNTs-Co<sup>o</sup>C, at 2.93 mg L<sup>-1</sup> initial Ni<sup>2+</sup> concentration and pH 7.0. It was observed from the Figure 8a that increasing the temperature increased the equilibrium adsorption capacity of Ni<sup>2+</sup> onto MMWCNTs-C, indicating the endothermic nature of the adsorption reaction.

In order to study the thermodynamics of adsorption of Ni<sup>2+</sup> onto MMWCNTs-C, three basic thermodynamic parameters, enthalpy ( $\Delta H^{\circ}$ ), entropy ( $\Delta S^{\circ}$ ) and Gibbs free energy ( $\Delta G^{\circ}$ ) were calculated using the following equations<sup>36</sup>:

$$\ln K_e = \frac{\Delta S^{\circ}}{R} - \frac{\Delta H^{\circ}}{R \cdot T} \quad (8)$$

$$K_a = \frac{q_e}{C_e} \quad (9)$$

$$\Delta G^{\circ} = -RT \ln K_a \quad (10)$$

where T (K) is the solution temperature, K<sub>a</sub> is the adsorption equilibrium constant, R (8.314 J mol<sup>-1</sup> K<sup>-1</sup>) is the gas constant. Enthalpy ( $\Delta H^{\circ}$ ) and entropy ( $\Delta S^{\circ}$ ) were calculated from the slope and intercept of van't Hoff plot of ln q<sub>e</sub>/C<sub>e</sub> versus 1/T (Fig. 8b). As it is shown, the obtained van't Hoff plot was linear with good correlation coefficient (R<sup>2</sup> = 0.985). The value of Gibbs free energy ( $\Delta G^{\circ}$ ) was calculated using Eq. 10. The values of  $\Delta H^{\circ}$ ,  $\Delta S^{\circ}$  and  $\Delta G^{\circ}$  are listed in Table 4. The positive value of  $\Delta H^{\circ}$  indicate that the adsorption process is an endothermic in nature. Kara et al.<sup>37</sup> suggested that the  $\Delta H^{\circ}$  of physisorption is smaller than 40 kJ mol<sup>-1</sup>. Thus, the values of  $\Delta H^{\circ}$  suggests that the adsorption of Ni<sup>2+</sup> onto MMWCNTs-C is a physisorption process. The positive value of  $\Delta S^{\circ}$  indicates that the degrees of freedom increased at the solid/solution interface during the adsorption of Ni<sup>2+</sup> onto MMWCNTs-C. The values of Gibbs free energy ( $\Delta G^{\circ}$ ) were negative in the temperature range of 20–60°C confirming that the adsorption was spontaneous and thermodynamically favorable. Similar results for the adsorption of Ni<sup>2+</sup> have been also reported in the literature using other adsorbents as activated carbon prepared from Thespesia Populnea bark<sup>38</sup> or magnetic nanoparticle (Fe<sub>3</sub>O<sub>4</sub>) impregnated onto tea waste<sup>5</sup>. The change in Gibbs free energy for physisorption is between -20 and 0 kJ mol<sup>-1</sup>, the physisorption together with chemisorptions is at the range of -20 to -80 kJ mol<sup>-1</sup> and chemisorption is at the range of -80 to -400 kJ mol<sup>-1</sup>. The values of  $\Delta G^{\circ}$  for the adsorp-

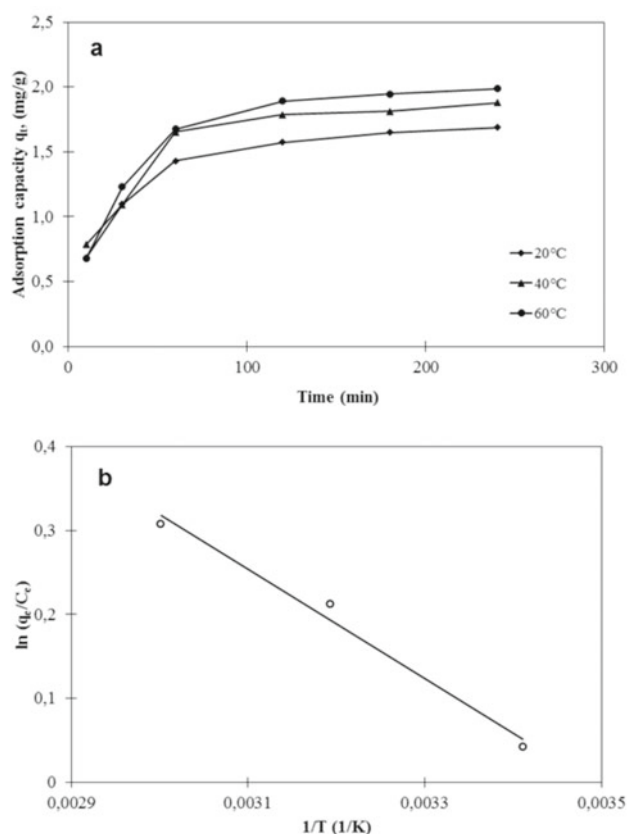


**Figure 8.** (a) Effect of temperature on adsorption of the  $\text{Ni}^{2+}$  onto MMWCNTs-C; (Experimental conditions:  $C_{\text{O},\text{Ni}^{2+}} = 2.93 \text{ mg L}^{-1}$ ,  $\text{pH} = 7.0$ ). (b) Van't Hoff plot for the adsorption of the  $\text{Ni}^{2+}$  onto MMWCNTs-C

tion of  $\text{Ni}^{2+}$  onto MMWCNTs-C were in the range of physisorption.

## CONCLUSIONS

In summary, a magnetic multiwalled carbon nanotubes nanocomposite MMWCNTs-C was synthesized by chemical vapor deposition CVD and was used as adsorbent for the removal of  $\text{Ni}^{2+}$  from aqueous solutions. The MMWCNTs-C adsorbent consists of magnetic particles and could be easily recovered by the magnetic separation method. The adsorption isotherm data were fitted well with the Langmuir model. The maximum monolayer adsorption capacity was  $2.11 \text{ mg g}^{-1}$ . Adsorption kinetics of  $\text{Ni}^{2+}$  onto MMWCNTs-C followed the pseudo-second-order kinetic model. The thermodynamic parameters ( $\Delta H^\circ$ ,  $\Delta G^\circ$  and  $\Delta S^\circ$ ) showed that the adsorption process of  $\text{Ni}^{2+}$  onto MMWCNTs-C was a spontaneous and endothermic process. Additionally, the adsorption of  $\text{Ni}^{2+}$  onto MMWCNTs-C was via a physisorption process.

## LITERATURE CITED

1. Krishna, R.H. & Swamy, A. (2011). Kinetic and isotherm modeling of adsorption of Ni (II) from aqueous solutions onto powder of papaya seeds. *Int. J. Sci. Res. Publ.* 1(1), 1–6.
2. Al-Asheh, S., Banat, F. & Mobai, F. (1999). Sorption of copper and nickel by spent animal bones. *Chemosphere* 39(12), 2087–2096.
3. Vijayaraghavan, K., Jegan, J., Palanivelu, K. & Velan, M. (2004). Removal of nickel(II) ions from aqueous solution using crab shell particles in a packed bed up-flow column. *J. Hazard. Mater.* B113, 223–230. DOI: 10.1016/j.jhazmat.2004.06.014.

4. Vijayaraghavan, K., Jegan, J., Palanivelu, K. & Velan, M. (2005). Biosorption of cobalt(II) and nickel(II) by seaweeds: batch and column studies. *Sep. Purif. Technol.* 44, 53–59. DOI: 10.1016/j.seppur.2004.12.003.
5. Panneerselvam, P., Morad, N. & Tan, K.A. (2011). Magnetic nanoparticle ( $\text{Fe}_3\text{O}_4$ ) impregnated onto tea waste for the removal of nickel(II) from aqueous solution. *J. Hazard. Mater.* 186, 160–168. DOI: 10.1016/j.jhazmat.2010.10.102.
6. Hasar, H. (2003). Adsorption of nickel(II) from aqueous solution onto activated carbon prepared from almond husk. *J. Hazard. Mater.* 97, 49–57. DOI: 10.1016/S0304-3894(02)00237-6.
7. Fiol, N., Villaescusa, I., Martinez, M., Miralles, N., Poch, J. & Serarols, J. (2006). Sorption of Pb(II), Ni(II), Cu(II) and Cd(II) from aqueous solution by olive stone waste. *Sep. Purif. Technol.* 50, 132–140. DOI: 10.1016/j.seppur.2005.11.016.
8. Rao, M., Parwate, A.V. & Bhole, A.G. (2002). Removal of  $\text{Cr}^{6+}$  and  $\text{Ni}^{2+}$  from aqueous solution using bagasse and fly ash. *Waste Manage.* 22, 821–830.
9. Tofighy, M.A. & Mohammadi, T. (2011). Adsorption of divalent heavy metal ions from water using carbon nanotube sheets. *J. Hazard. Mater.* 185, 140–147. DOI: 10.1016/j.jhazmat.2010.09.008.
10. Li, Y.H., Ding, J., Luan, Z., Di, Z., Zhu, Y., Xu, C., Wu, D. & Wei, B. (2003). Competitive adsorption of  $\text{Pb}^{2+}$ ,  $\text{Cu}^{2+}$  and  $\text{Cd}^{2+}$  ions from aqueous solutions by multiwalled carbon nanotubes. *Carbon* 41, 2787–2792. DOI: 10.1016/S0008-6223(03)00392-0.
11. Gao, Z., Bandosz, T.J., Zhao, Z., Han, M. & Qiu, J. (2009). Investigation of factors affecting adsorption of transition metals on oxidized carbon nanotubes. *J. Hazard. Mater.* 167, 357–365. DOI: 10.1016/j.jhazmat.2009.01.050.
12. Kandah, M.I. & Meunier, J.L. (2007). Removal of nickel ions from water by multi-walled carbon nanotubes. *J. Hazard. Mater.* 146(1–2), 283–288. DOI: 10.1016/j.jhazmat.2006.12.019.
13. Yang, S., Li, J., Shao, D., Hu, J. & Wang, X. (2009). Adsorption of Ni(II) on oxidized multi-walled carbon nanotubes: Effect of contact time, pH, foreign ions and PAA. *J. Hazard. Mater.* 166, 109–116. DOI: 10.1016/j.jhazmat.2008.11.003.
14. Chen, C., Hu, J., Shao, D., Li, J. & Wang, X. (2009). Adsorption behavior of multiwalled carbon nanotube/iron oxide magnetic composites for Ni(II) and Sr(II). *J. Hazard. Mater.* 164, 923–928. DOI: 10.1016/j.jhazmat.2008.08.089.
15. Jeon, S., Yun, J., Lee Y.S. & Kim, H.I. (2010). Removal of Cu(II) ions by Alginate/Carbon Nanotube/Maghemite Composite Magnetic Beads. *Carbon Lett.* 11(2), 117–121.
16. Gupta, V.K., Agarwal, S. & Saleh, T.A. (2011). Chromium removal by combining the magnetic properties of iron oxide with adsorption properties of carbon nanotubes. *Water Res.* 45(6), 2207–2212. DOI: 10.1016/j.watres.2011.01.012.
17. Ma, J., Zhu, Z., Chen, B., Yang, M., Zhou, H., Li, C., Yu, F. & Chen, J. (2013). One-pot, large-scale synthesis of magnetic activated carbon nanotubes and their applications for arsenic removal. *J. Mater. Chem. A* 1, 4662–4666. DOI: 10.1039/C3TA10329C.
18. Peng, X., Luan, Z., Di, Z., Zhang, Z. & Zhu, C. (2005). Carbon nanotubes-iron oxides magnetic composites as adsorbent for removal of Pb(II) and Cu(II) from water. *Carbon* 43(4), 880–883. DOI: 10.1016/j.carbon.2004.11.009.
19. Pelech, I. (2010). Preparation of carbon nanotubes using CVD method. *Pol. J. Chem. Tech.* 12(3), 45–49. DOI: 10.2478/v10026-010-0033-y.
20. Vijayaraghavan, K., Won, S.W. & Yun, Y.S. (2009). Treatment of complex Remazol dye effluent using sawdust- and coal-based activated carbons. *J. Hazard. Mater.* 167, 790–796. DOI: 10.1016/j.jhazmat.2009.01.055.
21. Sykuła-Zajac, A., Turek, M., Mathew, M.P., Patai, F., Horvat, M. & Jabłońska, J. (2010). Determination of nickel in tea by using dimethylglyoxime method. *Scientific Bulletin of the Technical University of Lodz. Food Chemistry and Biotechnology* 74(1081), 5–11.

22. Konicki, W., Pelech, I., Mijowska, E. & Jasińska, I. (2013). Adsorption Kinetics of Acid Dye Acid Red 88 onto Magnetic Multi-Walled Carbon Nanotubes-Fe<sub>3</sub>C Nanocomposite. *Clean-Soil, Air, Water*. In press. DOI: 10.1002/clen.201200458.

23. Chairat, M., Rattanaphani, S. & Bremner, J.B., Rattanaphani, V. (2008). Adsorption kinetic study of lac dyeing on cotton. *Dyes Pigm.* 76, 435–439. DOI: 10.1016/j.dyepig.2006.09.008.

24. Kumar, P.S. & Kirthika, K. (2009). Equilibrium and kinetic study of adsorption of nickel from aqueous solution onto bael tree leaf powder. *J. Eng. Sci. Technol.* 4(4), 351–363.

25. Ai, L., Zhou, Y. & Jiang, J. (2011). Removal of methylene blue from aqueous solution by montmorillonite/CoFe<sub>2</sub>O<sub>4</sub> composite with magnetic separation performance. *Desalination* 266, 72–77. DOI: 10.1016/j.desal.2010.08.004.

26. Kapoor, A. & Viraragavan, T. (1998). Heavy metal biosorption sites in *Aspergillus Niger*. *Bioresour. Technol.* 61, 221–227.

27. Kadivelu, K., Thamariselvi, K. & Namasivayam, C. (2001). Adsorption of Ni(II) from aqueous solution onto activated carbon prepared from Coirpith. *Sep. Purif. Technol.* 124, 497–505.

28. Suemitsu, R., Uenishi, R., Akashi, I. & Kakano, M. (1986). The use of dyestuff-treated rice hulls for removal of heavy metals from wastewater. *J. Appl. Polym. Sci.* 31, 74–83.

29. Al-Rub, F.A.A., Kandah, M. & Aldabaibeh, N. (2002). Nickel removal from aqueous solution by using sheep Manure Waste. *Eng. Life Sci.* 2, 111–116. DOI: 10.1002/1618-2863(200204).

30. Padmavathy, V. (2008). Biosorption of Ni(II) ions on Baker's yeast: kinetic, thermodynamic and desorption studies. *Bioresour. Technol.* 99, 3100–3109. DOI: 10.1016/j.biortech.2007.05.070.

31. Ho, Y.S., Jhonwase, D.A. & Forster, C.F. (1995). Batch nickel removal from aqueous solution by Sphagnum moss peat. *Water Res.* 29, 1327–1332.

32. Ewecharoen, A., Thiravetyan, P. & Nakbanpote, W. (2008). Comparison of nickel adsorption from electroplating rinse water by coir pith and modified coir pith. *Chem. Eng. J.* 137, 181–188. DOI: 10.1016/j.cej.2007.04.007.

33. Huang, C., Ying-Chien, C. & Ming-Ren, L. (1996). Adsorption of Cu(II) and Ni(II) by palletized biopolimer. *J. Hazard. Mater.* 45, 265–267.

34. Sharma, Y.C. & Srivastava, V. (2010). Separation of Ni(II) ions from aqueous solutions by magnetic nanoparticles. *J. Chem. Eng. Data* 55, 1441–1442. DOI: 10.1021/je900619d.

35. Meena, A.K., Mishra, G.K., Rai, P.K., Rajgopal, C. & Nagar, P.N. (2005). Removal of heavy metal ions from aqueous solution using carbon aerogel as an adsorbent. *J. Hazard. Mater.* 122, 161–170. DOI: 10.1016/j.jhazmat.2005.03.024.

36. Karagoz, S., Tay, T., Ucar, S. & Erdem, M. (2008). Activated carbons from waste biomass by sulfuric acid activation and their use on methylene blue adsorption. *Bioresour. Technol.* 99, 6214–6222. DOI: 10.1016/j.biortech.2007.12.019.

37. Kara, M., Yuzer, H., Sabah, E. & Celik, M.S. (2003). Adsorption of cobalt from aqueous solutions onto sepiolite. *Water Res.* 37, 224–232.

38. Prabakaran, R. & Arivoli, S. (2012). Adsorption kinetics, equilibrium and thermodynamic studies of Nickel adsorption onto *Thespesia Populnea* bark as biosorbent from aqueous solutions. *Euro. J. Appl. Eng. Sci. Res.* 1(4), 134–142.

39. Jaycock, M.J. & Parfitt, G.D. (1981). *Chem. Interf.* Ellis Horwood Ltd., Onichester.